Journal Pre-proof

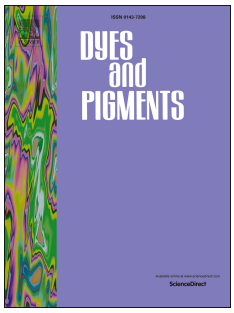

Synthesis of 2,6,9-substituted xanthen-3-one and solvent effect on structural and photophysical properties

Taro Koide, Shohei Iwamori, Satoshi Koga, Yasutaka Suzuki, Jun Kawamata, Yoshio Hisaeda

PII: S0143-7208(20)31364-4

DOI: https://doi.org/10.1016/j.dyepig.2020.108667

Reference: DYPI 108667

To appear in: *Dyes and Pigments*

Received Date: 10 March 2020

Revised Date: 22 June 2020

Accepted Date: 23 June 2020

Please cite this article as: Koide T, Iwamori S, Koga S, Suzuki Y, Kawamata J, Hisaeda Y, Synthesis of 2,6,9-substituted xanthen-3-one and solvent effect on structural and photophysical properties, *Dyes and Pigments*, https://doi.org/10.1016/j.dyepig.2020.108667.

Taro Koide: Conceptualization, Methodology, Validation, Investigation, Data Curation, Writing - Original Draft, Writing - Review & Editing, Project administration, Funding acquisition, **Shohei Iwamori**: Validation, Formal analysis, Investigation, Visualization, **Satoshi Koga**: Validation, Investigation, **Yasutaka Suzuki**: Formal analysis, Funding acquisition, **Jun Kawamata**: Formal analysis, Resources, Supervision, **Yoshio Hisaeda**: Resources, Supervision, Project administration, Funding acquisition

Highlights

The donor-π-donor type 2,6,9-substituted xanthen-3-one was newly synthesized.

The keto-enol isomerization behavior was observed depending on the solvent polarity.

Twisted intramolecular charge transfer (TICT) occurs in this system due to the rotation of electron donating aryl group at 2-position of the xanthene skeleton in the excited state.

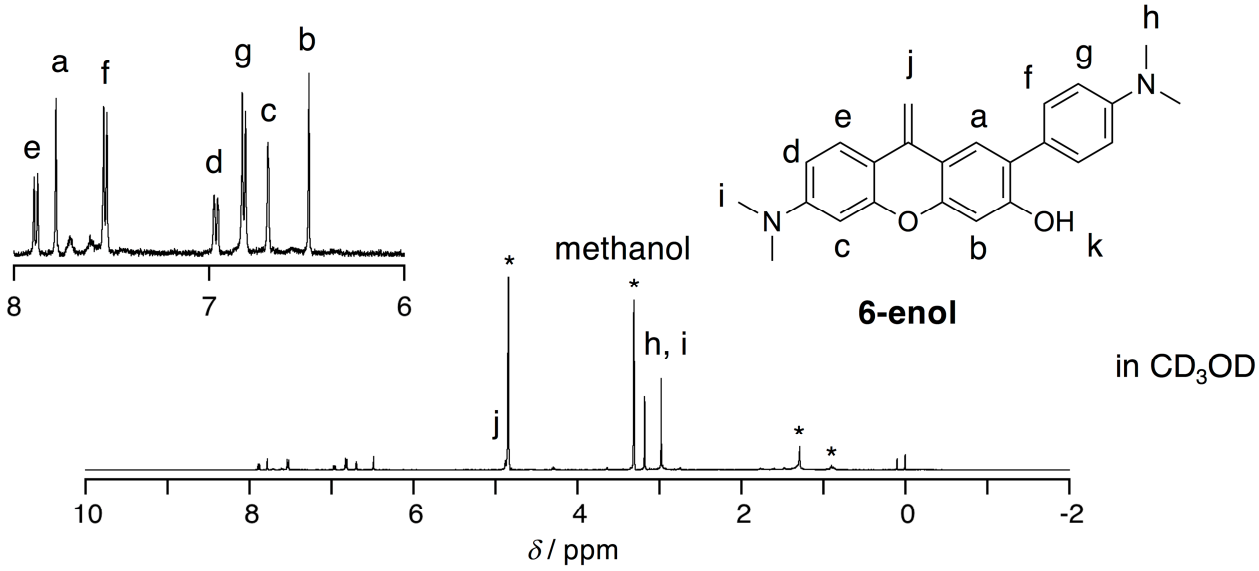

Figure. ^{1}H NMR spectrum of **6** in CD_3OD. *: solvents and impurities.

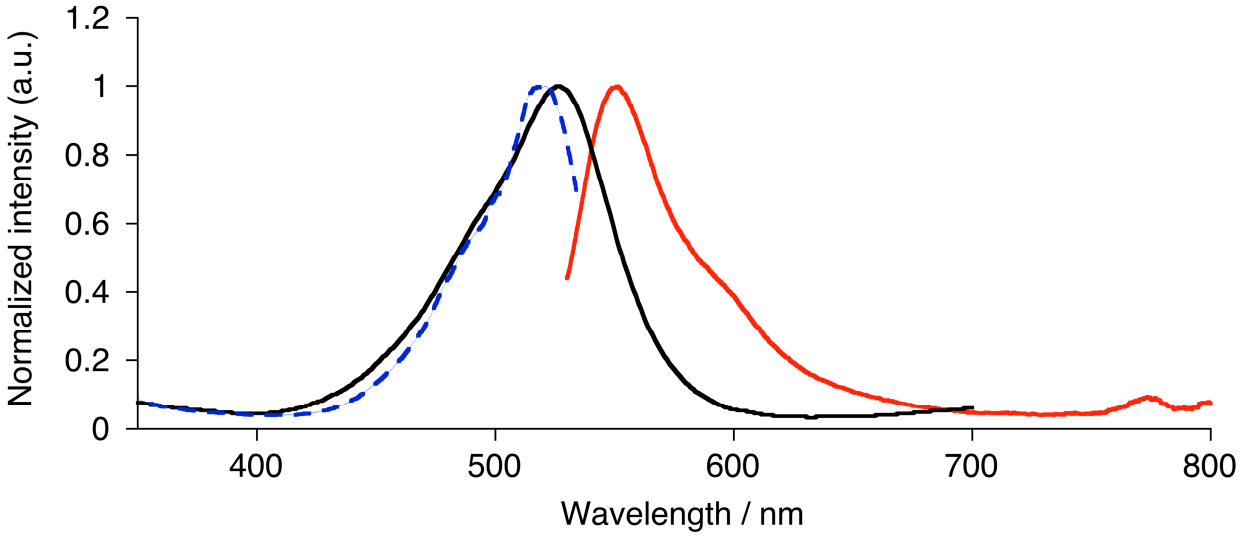

Figure. UV–vis absorption (black), fluorescence (red, excited at 510 nm), and excitation spectra of **6** (blue, dotted, monitored at 555 nm) in MeOH.

Synthesis of 2,6,9-substituted xanthen-3-one and solvent effect on structural and photophysical properties

Taro Koide,*[a] Shohei Iwamori,[a] Satoshi Koga,[b] Yasutaka Suzuki,[b] Jun Kawamata,[b] Yoshio Hisaeda*[a][c]

[a] Department of Chemistry and Biochemistry, Graduate School of Engineering, Kyushu University, Moto-oka 744, Nishi-ku, Fukuoka-shi, Fukuoka 819-0395, Japan

[b] Graduate School of Sciences and Technology for Innovation, Yamaguchi University, 1677-1 Yoshida, Yamaguchi, Yamaguchi 753-8512, Japan

[c] Center for Molecular Systems (CMS), Kyushu University, Moto-oka 744, Nishi-ku, Fukuoka-shi, Fukuoka 819-0395, Japan

Abstract

The synthesis of donor-π-donor type 2,6,9-substituted xanthen-3-one and its solvent effect on both the structural and photophysical properties were revealed. The keto-enol isomerization behavior and red-shift of the emission wavelengths were observed depending on the solvent polarity. This observation indicated that twisted intramolecular charge transfer (TICT) occurs in this system. This

is probably due to the electron donating aryl group at 2-position of the xanthene skeleton, which could rotate in the excited state. The luminescence of the compound was also confirmed in a living cell.

Keywords

xanthene, solvent effect, tautomerization, twisted intramolecular charge transfer (TICT)

1. Introduction

Fluorescence imaging has attracted many researchers since it can be used to monitor the surrounding environment of fluorescent molecules. [1-4] Especially, the molecules showing large Stokes shift could avoid the self-quenching and also could be possible to use the longer wavelength emission. The near infrared (NIR) light has high biopermeability and low scattering properties, which are advantageous not only in living systems but also in various medias. One of the methods to increase the Stokes shift is utilization of charge transfer (CT). Twisted intramolecular charge transfer (TICT) is the phenomenon induced by the photoexcitation and following twisting of the bond between the electron donor and acceptor, which highly depends on the solvent polarity and/or viscosity. TICT molecules exhibit red-shifted emission in the polar solvent due to the stabilization of the twisted charge separated excited state. [5,6]

Xanthene is known as the basic skeleton of a group of pigments, such as fluorescein, eosin, rhodamine, etc (Figure 1). Peripheral modification of the xanthene skeleton affords a variety of dyes. The selective modification of the chromophore is important to manipulate the electronic state of the molecule, affecting on the absorption and emission of the dyes. The development of synthetic methods of xanthene derivatives is well summarized in the recent review by Gryko and co-workers.[7] For the fluorescein derivatives, the importance of the benzene moiety at 9-position of xanthene skeleton and the substituent at ortho position of the benzene ring was revealed by Nagano and co-workers during the development of Tokyo Green.[8,9] The fixed perpendicular placement of xanthene backbone and benzene ring at 9-position is essential for high fluorescence quantum yield. They clarified that the increase of the electron donating property of 9-aryl group quenches the fluorescence via the photo-induced electron transfer to xanthene skeleton. However, there was no color change depending on the magnitude of the electron donating property of 9-aryl group and also on the steric hindrance of the *ortho* position of the aryl group. Non-radiative deactivation due to TICT state of rhodamines were discussed by Rettig and co-workers based on the 3,7-diamino substituted xanthene derivatives[10], however, it focused on the fluorescence quantum yield and deactivation process via non-emissive TICT state.

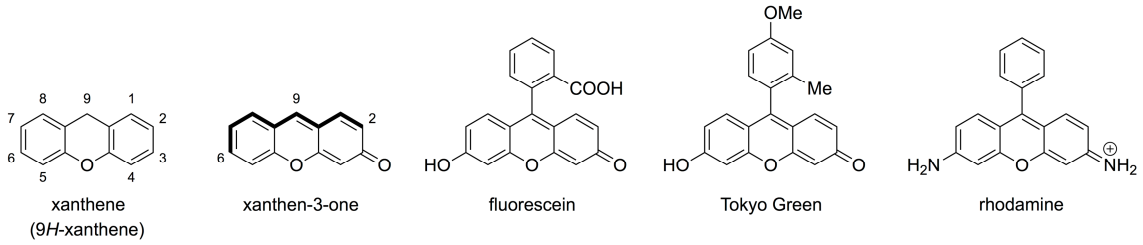

Figure 1. Structure of xanthene and known derivatives.

In this study, the synthesis of donor-π-donor type 2,6-substituted-9-methyl xanthen-3-one was achieved by the condensation of substituted precursors. The similar synthesis method had been reported, however the introduction of electron donating aryl group at 2-position had not been investigated. [11,12] The efficient synthetic method of 9-alkyl substituted xanthene derivatives has been improved in the past one or two decades,[7,12-15] though they had been used as lasing dyes for long time.[16] Among them, the 9-methyl substituted xanthenes are known to show the keto-enol tautomerization by the change in pH.[15] It was also described that the 9-methyl xanthene was converted to enol-form in the hydrogen-bond acceptor solvent DMSO to a large extent. In that case, the fluorescence intensity of keto-form was reported to be low, but the details of the solvent effect were not discussed. In this study, we focused on the 2- and 6-position substitution because these positions are on the diagonal of the molecular skeleton of xanthene, which are expected to afford the effective π-conjugation connected to the terminal substituents. 6-dimetylamino, 2-dimetylaminophenyl substituted 9-methyl xanthen-3-one was synthesized and investigated the detailed spectroscopic charcterizations to find unique structural and electronic properties of the

compound. The keto-enol tautomerization was confirmed by the NMR measurements in various solvents. We also found that effective TICT emission was observed in the solvents that do not form hydrogen bonding.

2. Materials and Methods

As a precursor, 4-bromoresorcinol **1** was selected. Benzyl protection of the hydroxyl groups of **1** gave compound **2**. Following Suzuki-Miyaura cross coupling with 4-dimethylaminophenyl boronic acid pinacol ester gave 4-(4-dimethylaminophenyl) resorcinol derivative **3**. Deprotection of benzyl groups afforded the precursor **4**. The condensation of **4** and **5** in methane sulfonic acid afforded the target compound, 2,6,9-substituted xanthen-3-one **6** in 72% yield (Scheme 1).

Characterization of the compounds **3**, **4**, and **6** was performed by ^{1}H NMR, ^{13}C NMR, HR-ESI-TOF-MS. (SI) Compound **5** was synthesized according to the reported method. [12]

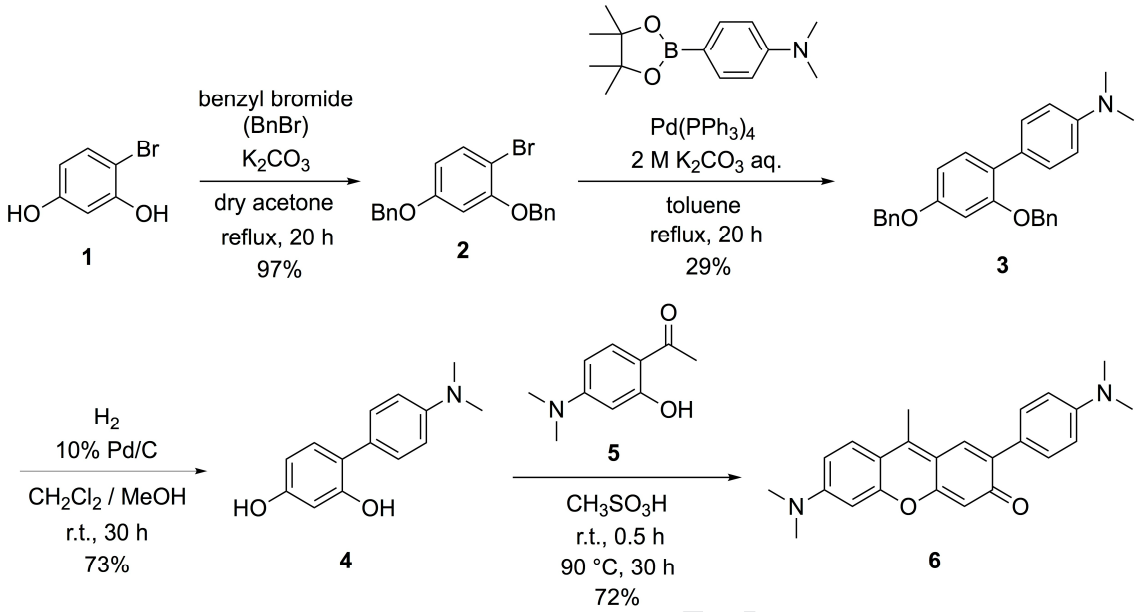

Scheme 1. Synthesis of 2,6-substituted-9-methyl xanthene **6**.

3. Results and Discussions

2-Dimethylaminophenyl-6-dimethylaminio substituted xanthene **6** exhibited remarkable solvent effects; one was the keto-enol tautomerization and the other was the change of emission based on TICT. From a structural viewpoint, the keto-enol (quinoid-benzenoid) tautomerization at 3- and 9-position of xanthene was observed in the ^{1}H NMR spectra. In $CDCl_3$, the signal, which could be assigned as the proton of methyl group at 9-position of xanthene, was observed at 2.63 ppm, indicating that **6** took keto-form, **6-keto** (Figure 2a, Figure S7). On the contrary, in DMSO-d_6, the signal of terminal olefin was observed at 5.23 ppm along with the signal of terminal OH-proton at 9.90 ppm, indicating that the xanthene **6** took the enol-form, **6-enol** (Figure 2c). The proportions of keto-form and enol-form were checked in various solvents (Figure 2, Figure S9-S14, Table 1) and

were calculated from the integral intensities of the signals in ^{1}H NMR. In acetone, benzene, and toluene, keto- and enol-forms co-existed in the ratio of 58:42, 79:21, and 79:21, respectively. Based on the results, the enol-from seemed to be stabilized by the interaction between the OH-proton of the hydroxyl group at 3-position and the solvents; hydrogen bonding for DMSO, DMF and acetone and O-H-π interaction for benzene and toluene.

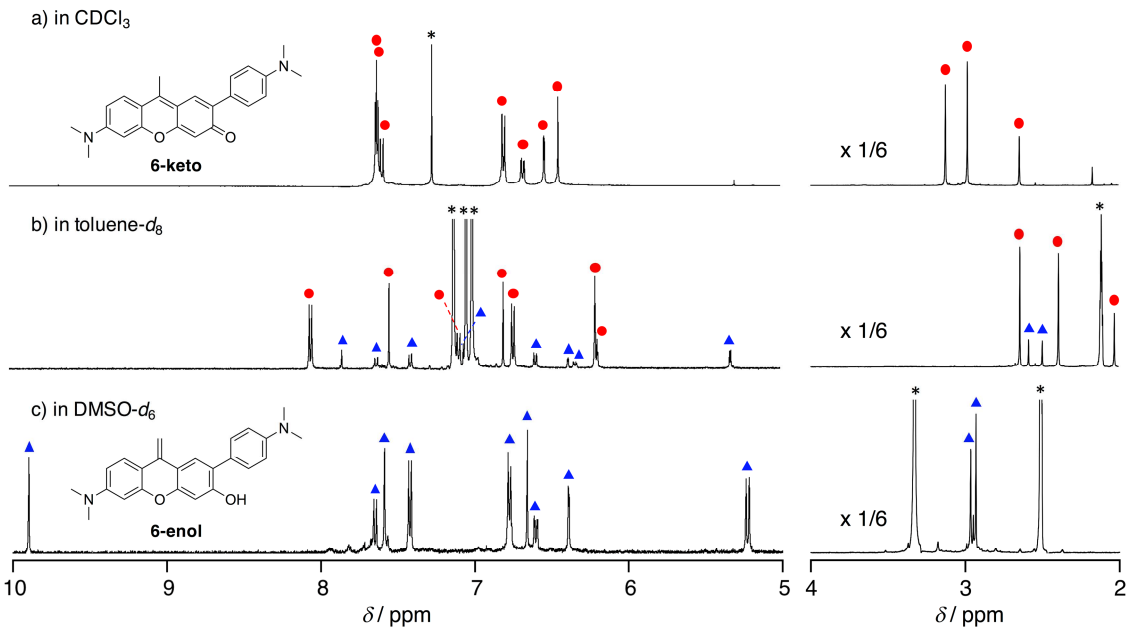

Figure 2. Comparison of ^{1}H NMR spectra of **6 in** a) $CDCl_3$, b) toluene-d_8, and c) DMSO-d_6. The signals assigned to **6-keto** are labeled with red circle, and those assigned to **6-enol** are labeled with blue triangle.

The UV-vis absorption, fluorescence, and fluorescence quantum yield of compound **6** were measured in benzene, toluene, chloroform, dichloromethane, acetone, DMF, and DMSO (Figure 3-5,

Figure S15-21, Table 1). The absorption spectra showed the absorption maxima around 500 and 520 nm in almost all the solvents. However, a large solvent effect was observed for the fluorescence spectra and fluorescence quantum yields. In DMF and DMSO, the observed emission wavelength was at 565 nm and 567 nm with the small Stokes shifts of 1276 and 1196 cm^{-1}, respectively (Figure S20, S21) and their fluorescence quantum yields were 1.2 and 1.3 %, indicating that the enol-form **6-enol** does not emit strongly and there was a small energy relaxation in the excited state. On the other hand, the fluorescence wavelength in benzene was observed at 624 nm, while that in chloroform was observed at 670 nm and in acetone at 685 nm. Thus, it has been confirmed that the Stokes shift values are significantly different. In addition, the fluorescence quantum yield was 40% in benzene, whereas it was 17% in chloroform and 3% in acetone. We considered that the difference in the Stokes shift values is due to the twisted intramolecular charge transfer (TICT). [5,6] Therefore, we evaluated the solvent polarity shown in the table and Lippert-Mataga plot. The solvent polarity parameter $\Delta f = (\varepsilon\text{-}1/2\varepsilon+1)\text{-}(n^2\text{-}1/2n^2+1)$ (ε: relative permittivity, n: refractive index) and the Stokes shifts showed a linear correlation, indicating the TICT fluorescence of the molecule (Figure 6). The fluorescence quantum yield and the solvent polarity also showed linear correlations (Figure4, Table 1, Figure S22), which supported the fact that the non-radiative deactivation process of the excited state is enhanced in a polar solvent. Compared to the examples of fluorescein and rhodamine, which possess aryl groups at 9-position, the effect of solvents is remarkably large in this molecule. This is

probably due to the difference in the energy barrier for the rotation of the aryl group. The rotation barrier of the phenyl ring on biphenyl and phenyl anthracene had been known to be ~2-3 and ~21 kcal/mol, respectively. [17][18] TICT and non-radiative deactivation probably occurred due to the rotation of the aryl ring.

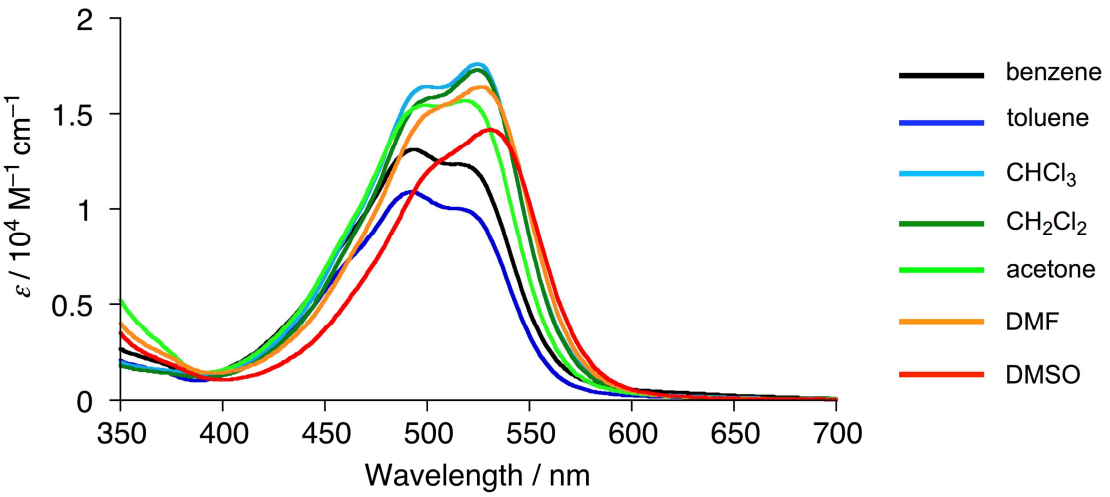

Figure 3. UV-vis absorption spectra of **6** in various solvents.

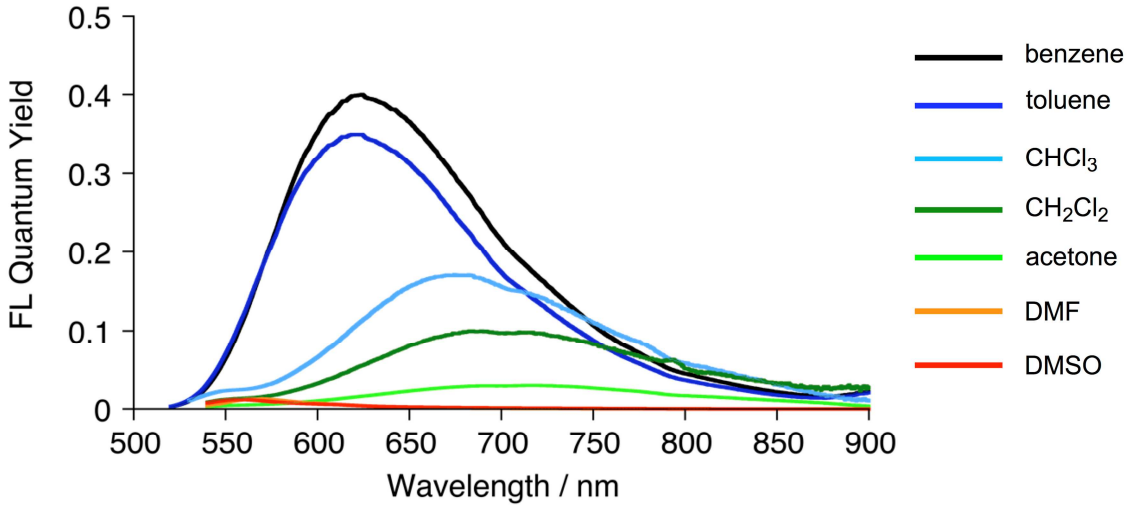

Figure 4. Emission spectra of **6** in various solvents.

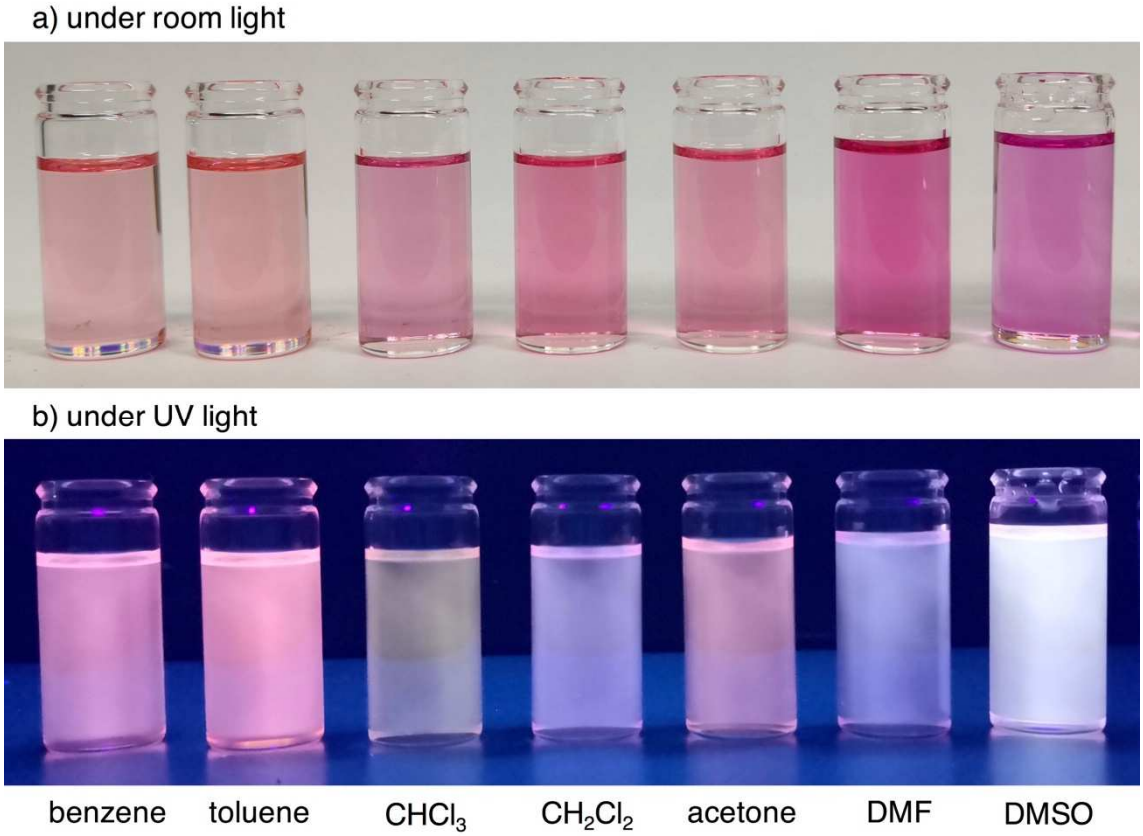

Figure 5. Photo image of the solutions of **6** in various solvents under room light and under UV light. Concentrations of the solutions were ~2 x 10^{-5} M.

Table 1. Comparison of the optical properties of **6** in various solvents

solvent	solvent polarity (Δf)	absorption (λ_{max}/ nm)	Emission (λ_{max}/ nm)	Stokes shift (cm^{-1})	FLQY	FL life time (/ ns)
benzene	0.00294	494, 515	624	3391	40% (51% [a])	2.6
toluene	0.0153	492, 514	621	3352	35% (44% [a])	2.5

$CHCl_3$	0.152	500, 524	670	4159	17%	2.0
CH_2Cl_2	0.220	502, 525	683	4406	10%	1.7
Acetone	0.284	499, 519	685	4669	3.0% (5.0% [a])	2.8
DMF	0.274	502 (sh), 527	565	1276	1.2%	3.4
DMSO	0.263	504 (sh), 531	567	1196	1.3%	3.3

a: The calculated FLQYs of **6-keto** from the existing ratio in a solution assuming that **6-enol** is non-emissive.

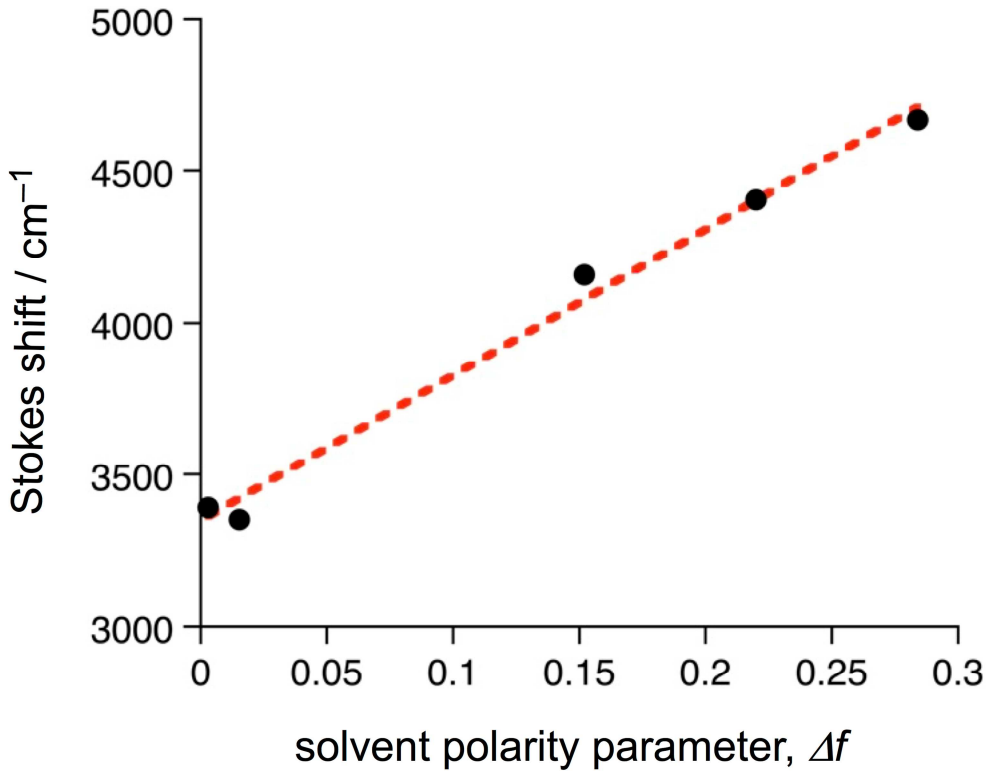

Figure 6. Lippert–Mataga plot of Stokes shifts for **6** vs. solvent polarity Δf for benzene, toluene, $CHCl_3$, CH_2Cl_2, and acetone.

Considering the red emission property of compound **6**, applicability as fluorescence probe for biological material was investigated. The fluorescence microscope image of HEK293 cell stained by compound **6** is shown in Figure 7. The fluorescence signal of green channel was the highest compared to other, blue or red, colored channels. This suggested that the TICT of **6** seemed to not occur in the living cell corresponding to the TICT that did not occur in polar solvents such as DMSO and DMF. By the way, a clear fluorescence microscope image was obtained by employing **6**. This observation indicated that **6** certainly exhibited fluorescence in cell and can be used as a fluorescence probe for microscopic observations in live cell. Considering the shape of the microscope image, compound **6** is thought to be localized on mitochondria (Figure 7, Figure S23). [19]

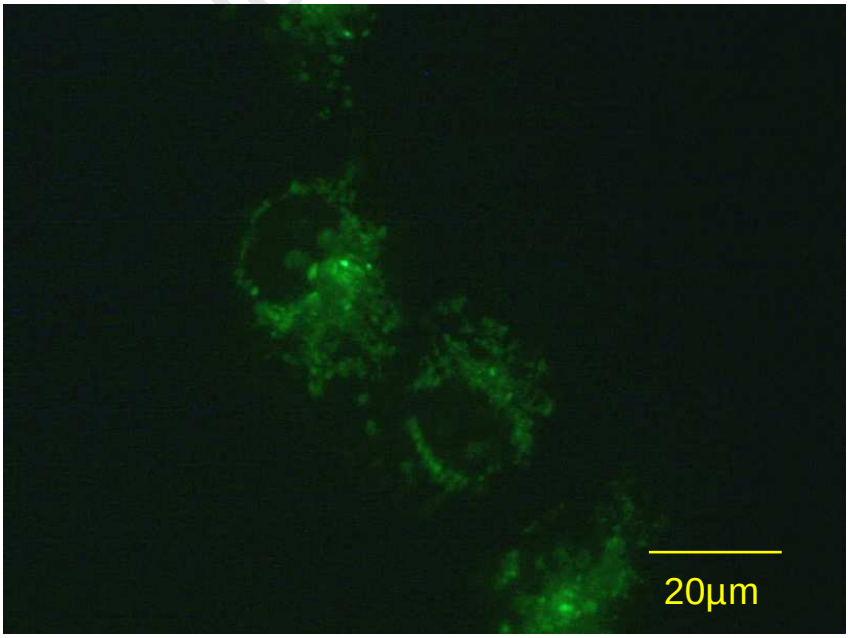

Figure 7. Fluorescence microscope images of living cells stained with **6**.

4. Conclusions

In summary, D-π-D type xanthene derivative **6** was successfully synthesized and the interesting solvent effects on the isomerization behavior and emission with a large Stokes shift raised from the TICT were revealed. Moreover, we confirmed that compound **6** could be used as a probe for fluorescence microscope.

5. Acknowledgements

This work was partially supported by JSPS KAKENHI Grant Number JP19K22204, 19K05403, 19H04677. T. K. is grateful for the financial support from Tonen General Sekiyu, CASIO SCIENCE PROMOTION FOUNDATION and Kyushu University.

6. References

[1] A. P. de Silva, H. Q. N. Gunaratne, T. Gunnlaugsson, A. J. M. Huxley, C. P. McCoy, J. T. Rademacher, T. E. Rice, *Chem. Rev.* **1997**, *97*, 1515−1566. https://doi.org/10.1021/cr960386p

[2] Z. Guo, S. Park, J. Yoon, I. Shin, *Chem. Soc. Rev.* **2014**, *43*, 16−29. https://doi.org/10.1039/C3CS60271K

[3] L. Wang, W. Du, Z. Hu, K. Uvdal, L. Li, W. Huang, *Angew. Chem. Int. Ed.* **2019**, *58*, 14026−14043. https://doi.org/10.1002/anie.201901061

[4] L. Wang, M. S. Frei, A. Salim, K. Johnsson, *J. Am. Chem. Soc.* **2019**, *141*, 2770−2781. https://doi.org/10.1021/jacs.8b11134

[5] D. Liese, G. Haberhauer, *Isr. J. Chem.* **2018**, *58*, 813−826. https://doi.org/10.1002/ijch.201800032

[6] S. Sasaki, G. P. C. Drummen, G. Konishi, *J. Mater. Chem. C* **2016**, *4*, 2731−2743. https://doi.org/10.1039/C5TC03933A

[7] Y. M. Poronik, K. V. Vygranenko, D. Gryko, D. T. Gryko, *Chem. Soc. Rev.* **2019**, *48*, 5242−5265. https://doi.org/10.1039/C9CS00166B

[8] Y. Urano, M. Kamiya, K. Kanda, T. Ueno, K. Hirose, T. Nagano, *J. Am. Chem. Soc.* **2005**, *127*, 4888−4894. https://doi.org/10.1021/ja043919h

[9] M. Kamiya, H. Kobayashi, Y. Hama, Y. Koyama, M. Bernardo, T. Nagano, P. L. Choyke, Y. Urano, *J. Am. Chem. Soc.* **2007**, *129*, 3918−3929. https://doi.org/10.1021/ja067710a

[10] M. Vogel, W. Rettig, R. Sens, K. H. Drexhage, *Chem. Phys. Lett.* **1988**, *147*, 452−460. https://doi.org/10.1016/0009-2614(88)85007-3

[11] R. R. Sauers, S. N. Husain, A. P. Piechowski, G. R. Bird, *Dyes and Pigments*, **1987**, *8*, 35−53. https://doi.org/10.1016/0143-7208(87)85004-0

[12] Ye. M. Poronik, M. P. Shandura, Yu. P. Kovtun, *Dyes and Pigments* **2007**, *72*, 199−207. https://doi.org/10.1016/j.dyepig.2005.08.017

[13] Á. Martínez-Peragón, D. Miguel, R. Jurado, J. Justicia, J. M. Álvarez-Pez, J. M. Cuerva, L. Crovetto, *Chem. Eur. J.* **2014**, *20*, 447−455. https://doi.org/10.1002/chem.201303113

[14] M. Gangopadhyay, R. Mengji, A. Paul, Y. Venkatesh, V. Vangala, A. Jana, N. D. P. Singh, *Chem. Commun.* **2017**, *53*, 9109−9112. https://doi.org/10.1039/C7CC03241B

[15] P. Šebej, J. Wintner, P. Müller, T. Slanina, J. A. Anshori, L. A. P. Antony, P. Klán, J. Wirz, *J. Org. Chem.* **2013**, *78*, 1833−1843. https://doi.org/10.1021/jo301455n

[16] A. P. Piechowski, G. R. Bird, *Optics Communications*, **1984**, *50*, 386−392. https://doi.org/10.1016/0030-4018(84)90107-X

[17] F. Grein, *J. Phys. Chem. A* **2002**, *106*, 3823−3827. https://doi.org/10.1021/jp0122124

[18] K. Nikitin, H. Müller-Bunz, Y. Ortin, J. Muldoon, M. J. McGlinchey, *Org. Lett.* 2011, *13*, 256−259. https://doi.org/10.1021/ol102665y

[19] Y. Niko, H. Moritomo, H. Sugihara, Y. Suzuki, J. Kawamata, G. Konishi, *Journal of Materials Chemistry B* **2015**, *3*, 184−190. https://doi.org/10.1039/C4TB01404A

Supporting Information

Synthesis of 2,6,9-substituted xanthen-3-one and solvent effect on structural and photophysical properties

Taro Koide,*[a] Shohei Iwamori,[a] Satoshi Koga,[b] Yasutaka Suzuki,[b] Jun Kawamata,[b] Yoshio Hisaeda*[a][c]

[a] Department of Chemistry and Biochemistry, Graduate School of Engineering, Kyushu University, Moto-oka 744, Nishi-ku, Fukuoka-shi, Fukuoka 819-0395, Japan

[b] Graduate School of Sciences and Technology for Innovation, Yamaguchi University, 1677-1 Yoshida, Yamaguchi, Yamaguchi 753-8512, Japan

[c] Center for Molecular Systems (CMS), Kyushu University, Moto-oka 744, Nishi-ku, Fukuoka-shi, Fukuoka 819-0395, Japan

Contents

1. General information

Reagents and solvents of the best grade available were purchased from commercial suppliers and were used without further purification unless otherwise noted. Dried acetone was obtained by distillation from CaH_2 under a N_2 atmosphere.

Nuclear magnetic resonance (NMR) spectra were recorded on a Bruker Avance 500MHz NMR spectrometer. The resonance frequencies are 500 MHz for ^{1}H and 125 MHz for ^{13}C. Chemical shifts were reported as δ values in ppm relative to solvent residual solvents.[S1] High-resolution electron spray ionization mass spectra (HR-ESI-TOF-MS) were measured and recorded on an micrOTOFQII spectrometer (Bruker). Ultraviolet–visible–near infrared (UV–vis–NIR) absorption spectra were recorded on U-3310 spectrometer (Hitachi, Japan) and UV-3150PC (Shimadzu). Fluorescence excitation and emission spectra were collected at room temperature on a Hitachi F-7000 fluorescence spectrometer. Fluorescence spectra of 6 in DMF and DMSO were recorded by FP-8300 (JASCO Co.). Emission spectra were collected with a scan speed of 240 nm/min, and the slits were set at 2.5 nm (excitation slit) and 2.5 nm (emission slit). The absolute photoluminescence quantum yields (Φ_{PL}) were determined using absolute PL quantum yields measurement system C9920-02 (Hamamatsu photonics). Time-resolved photoluminescence lifetimes were carried out by using time-correlated single-photon counting lifetime spectroscopy system, Quantaurus-Tau C11367-02 (Hamamatsu photonics). The decay constants and fitting parameters for transient decays were determined using the embedded software of Quantaurus-Tau.

2. Experimental Details.

Cell culture and fluorescence microscopy

HEK293 cells were grown in Dulbecco's modified Eagle medium (DMEM, Sigma-Aldrich Japan), supplemented with 10% fetal bovine serum (FBS, Sigma-Aldrich Japan) at 37 ℃ in a humidified atmosphere containing 5% CO_2. HEK293 cell were treated with medium containing 1 μM of compound **6** for 24 hours. For imaging, HEK293 cells were washed several times with phenol-red-free medium (Opti-MEM, Invitrogen) supplemented with 10% (v/v) FBS.

Fluorescence images were obtained via a wide-field fluorescencemicroscope IX81 (OLYMPUS) equipped with digital camera DP50 (OLYMPUS). Green emission of compound **6** was collected by U-MW1G (excitation filter 510-560 nm, dichroic mirror 565 nm, barrier filter 590 nm).

1,3-bis(benzyloxy)-4-Bromobenzene **2**

4-bromoresorcinol (1.0 g, 5.3 mmol) and potassium carbonate (1.61 g, 11.6 mmol) were added to a 100 mL two-necked flask. After purging with nitrogen, 30 mL of dehydrated acetone and benzyl bromide (1.4 mL, 11.6 mmol) were added. After refluxing for 20 h, the reaction solution was evaporated under reduced pressure,

extracted with dichloromethane, washed with brine, and dried under reduced pressure. **2** was obtained as yellowish brown solid (1.9 g, 97%) and used to the next reaction without further purification.

^{1}H NMR (500 MHz, $CDCl_3$): δ = 5.03 (s, 2H, -O$\underline{CH_2}$Ph), 5.13 (s, 2H, -O$\underline{CH_2}$Ph), 6.53(dd, 1H, J = 2.5 Hz, 9.0 Hz), 6.66 (d, 1H, J = 2.5 Hz), 7.3-7.6 (m, 15H) ppm, ^{13}C NMR (125 MHz, $CDCl_3$): δ = 70.38, 70.78, 102.59, 103.58, 107.67, 126.98, 127.44, 127.90, 128.08, 128.54, 128.59, 133.19, 136.39, 136.53, 155.72, 159.20 ppm

HR-MS (ESI-TOF, positive mode): $C_{20}H_{17}BrO_2$ ([M]$^+$) m/z found; 368.0418, calcd; 368.0406

1,3-bis(benzyloxy)-4-(4-dimethylaminophenyl)benzene **3**

Compound **2** (200 mg, 0.543 mmol) and 4-dimethylaminophenylboronic acid pinacol ester (160 mg, 0.65 mmol) were added to a 100 mL two-necked flask. Then, 50 mL of toluene and 10 mL of an aqueous potassium carbonate solution (2 M) were added under N_2 atmosphere. After nitrogen bubbling for 10 min, tetrakis(triphenylphosophine)palladium(0) (100 mg, 0.086 mmol) was added, and the mixture was stirred for 24 h under refluxing. The solvent was removed by distillation under reduced pressure, and the resulting mixture was separated by column chromatography (ethyl acetate: hexane = 3:97) to afford **3** as a white solid (65 mg, 29%).

^{1}H NMR (500 MHz, $CDCl_3$): δ = 2.99 (s, 6H, N($\underline{CH_3}$)$_2$), 5.06 (s, 4H, -O$\underline{CH_2}$Ph), 6.65 (dd, 1H, J = 2.5 Hz, 8.0 Hz), 6.68 (d, 1H, J = 2.5 Hz), 6.78 (d, 1H, J = 8.0 Hz), 7.3-7.6 (m, 13H) ppm, ^{13}C NMR (125 MHz, $CDCl_3$): δ = 41.10, 70.69, 70.96, 102.33, 106.99, 112.72, 125.13, 127.05, 127.39, 127.95, 127.98, 128.39, 128.84, 129.03, 130.58, 131.34, 137.57, 137.78, 149.82, 156.97, 159.09 ppm

HR-MS (ESI-TOF, positive mode): $C_{28}H_{27}NO_2$ ([M]$^+$) m/z found; 409.2026, calcd; 409.2036

4-(4-dimethylaminophenyl)resorcinol **4**

10% Pd/C (20 mg) was added to a 25 mL round-bottom flask, followed by purging with nitrogen. Thereto was added a solution of compound **3** (65 mg, 0.15 mmol) in 10 mL of dichloromethane / methanol = 1/1. The system was filled with a constant hydrogen pressure, followed by stirring at room temperature for 30 h. The reaction mixture was filtered through celite, washed with dichloromethane. The obtained solution was evaporated under reduced pressure. The resulting mixture was purified by column chromatography (ethyl acetate: hexane = 1: 5) to afford **4** as white crystals (25 mg, 73%).

^{1}H NMR (500 MHz, $CDCl_3$): δ = 3.00 (s, 6H,), 4.81 (s, 1 H), 5.34 (s, 1H), 6.44 (dd, 1H, J = 2.5 Hz, 8.0 Hz), 6.48 (d, 1H, J = 2.5 Hz), 6.83(d, 2H, J = 8.5 Hz), 7.05 (d, 1H, J = 8.0 Hz), 7.28 (d, 2H, J = 8.5 Hz) ppm, ^{13}C NMR (125 MHz, $CDCl_3$): δ = 40.49, 102.56, 107.77, 113.21, 121.38, 124.17, 129.86, 130.80, 150.06, 153.06, 153.73, 155.86 ppm

HR-MS (ESI-TOF, positive mode): $C_{14}H_{15}NO_2$ ([M+H]$^+$) m/z found; 230.1165, calcd; 230.1176

6-dimethylamino-2-(4-dimethylaminophenyl)-9-methylxanthen-3-one **6**

Into a 20 ml Schlenk tube, **4** (25 mg, 0.11 mmol) and 2-acethyl-5-dimethylaminophenol **5** (19 mg, 0.11 mmol) were added. After purging with nitrogen, 4 mL of methanesulfonic acid was added, and the mixture was stirred at room temperature for 30 min and then at 90 °C for 30 h. After cooling to room temperature, 50 mL of iced water was added, and neutralized with sodium bicarbonate. The crude mixture was extracted with dichloromethane, washed with brine, and dried over Na_2SO_4. The solution was concentrated under reduced pressure, and purified by silica gel column chromatography (dichlorometane) to afford **6** as a purple solid (30 mg, 72%).

^{1}H NMR (500 MHz, $CDCl_3$): δ = 2.63 (s, 3H), 2.98 (s, 6H), 3.11 (s, 6H), 6.44 (s, 1H) 6.53 (d, 1H, J = 3.0 Hz), 6.68 (dd, 1H, J = 3.0 Hz, 9.0 Hz), 6.80 (d, 2H, J = 9.5 Hz), 7.59 (d, 1H, J = 9.0 Hz), 7.61 (s, 1H), 7.62 (d, 2H, J = 9.5 Hz) ppm, ^{13}C NMR (125 MHz, $CDCl_3$): δ = 13.44, 40.13, 40.61, 97.43, 105.37, 109.63, 111.45, 112.33, 116.45, 124.98, 126.20, 126.64, 130.03, 138.21, 144.91, 150.31, 153.59, 154.44, 157.86, 183.58 ppm

HR-MS (ESI-TOF, positive mode): $C_{24}H_{24}N_2O_2$ ($[M+H]^+$) m/z found; 373.1896, calcd; 373.1911, UV-vis (CH_2Cl_2): λ_{max}/nm (ε/M^{-1} cm^{-1}): 525 (17300) , FL (CH_2Cl_2, excited at 525 nm): λ_{max}/nm 683, Stokes shift: 158 nm, 4406 cm^{-1}, quantum yield (φ_{fl}): 10%, excited state lifetime (τ): 1.7 ns.

3. NMR spectra

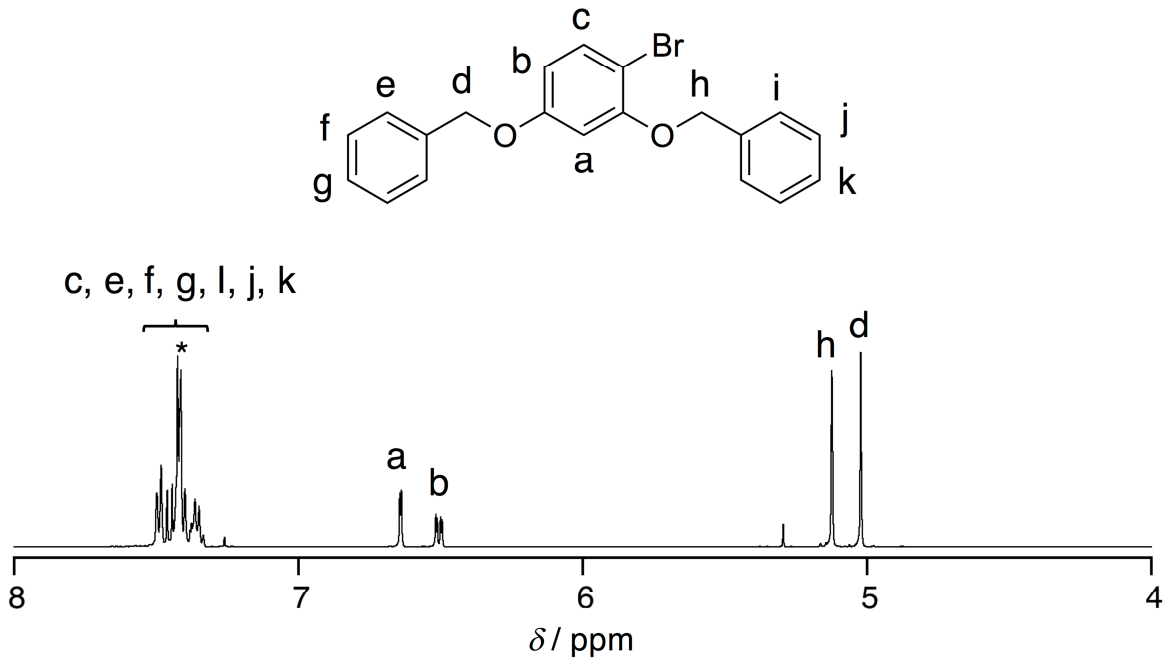

Figure S1. ^{1}H NMR spectrum of **2** in $CDCl_3$. *: solvents and impurities.

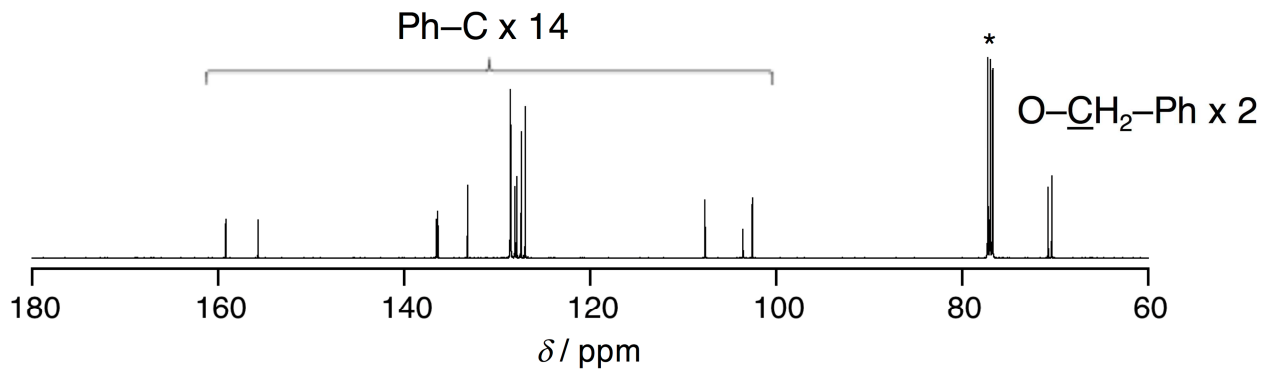

Figure S2. ^{13}C NMR spectrum of **2** in $CDCl_3$. *: solvents and impurities.

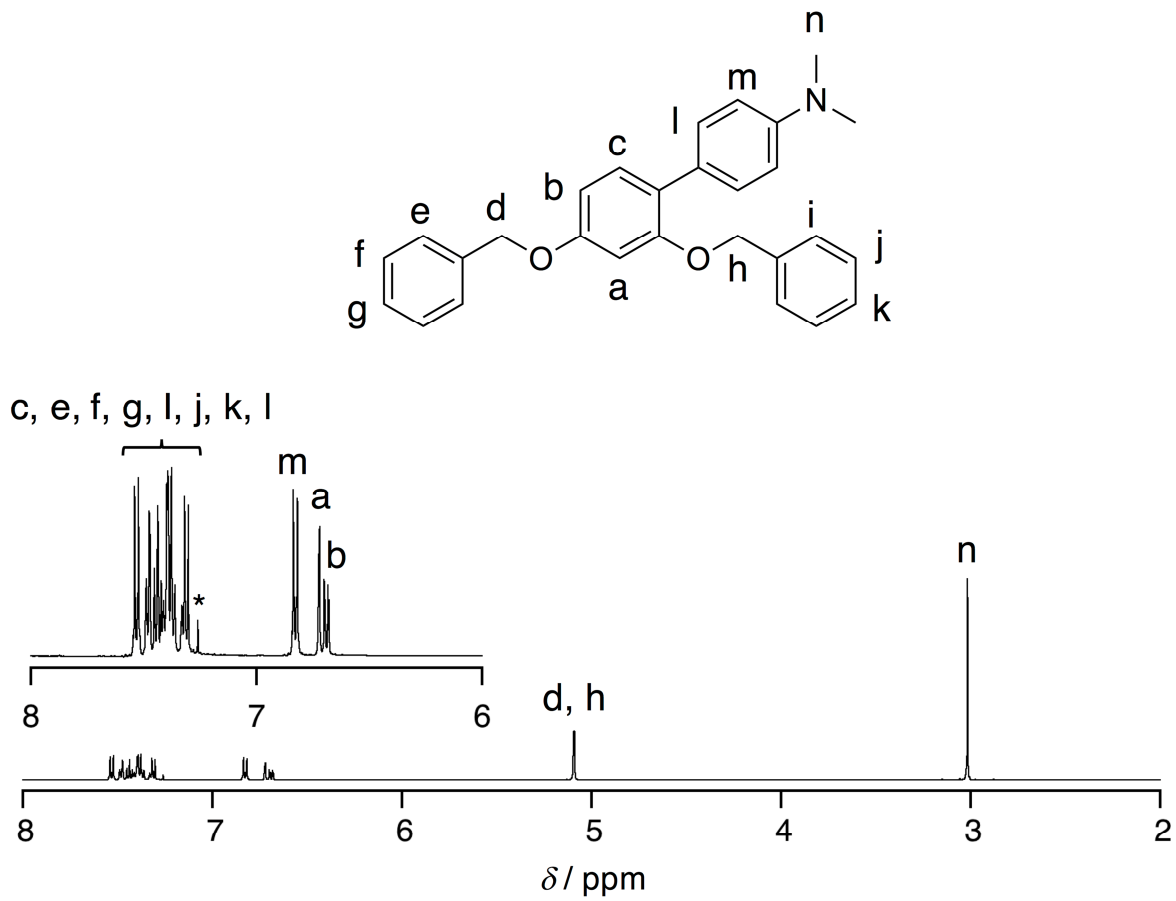

Figure S3. ^{1}H NMR spectrum of **3** in $CDCl_3$. *: solvents and impurities.

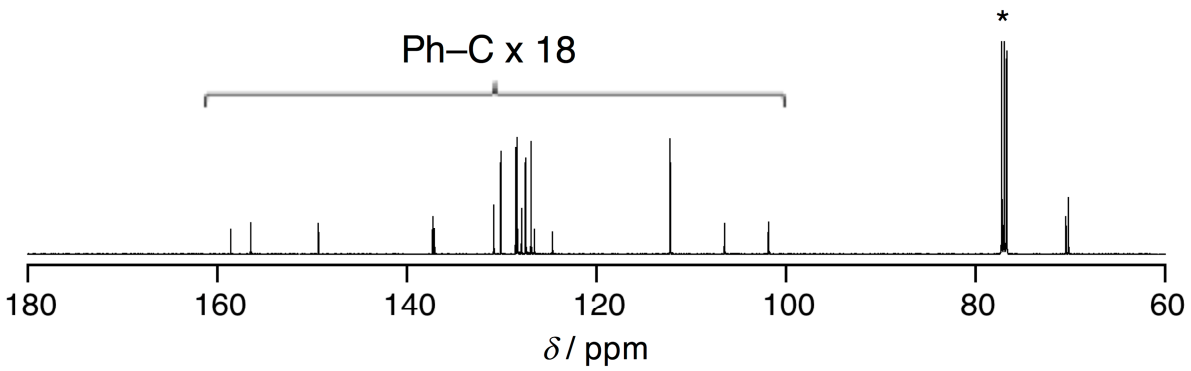

Figure S4. ^{13}C NMR spectrum of **3** in $CDCl_3$. *: solvents and impurities.

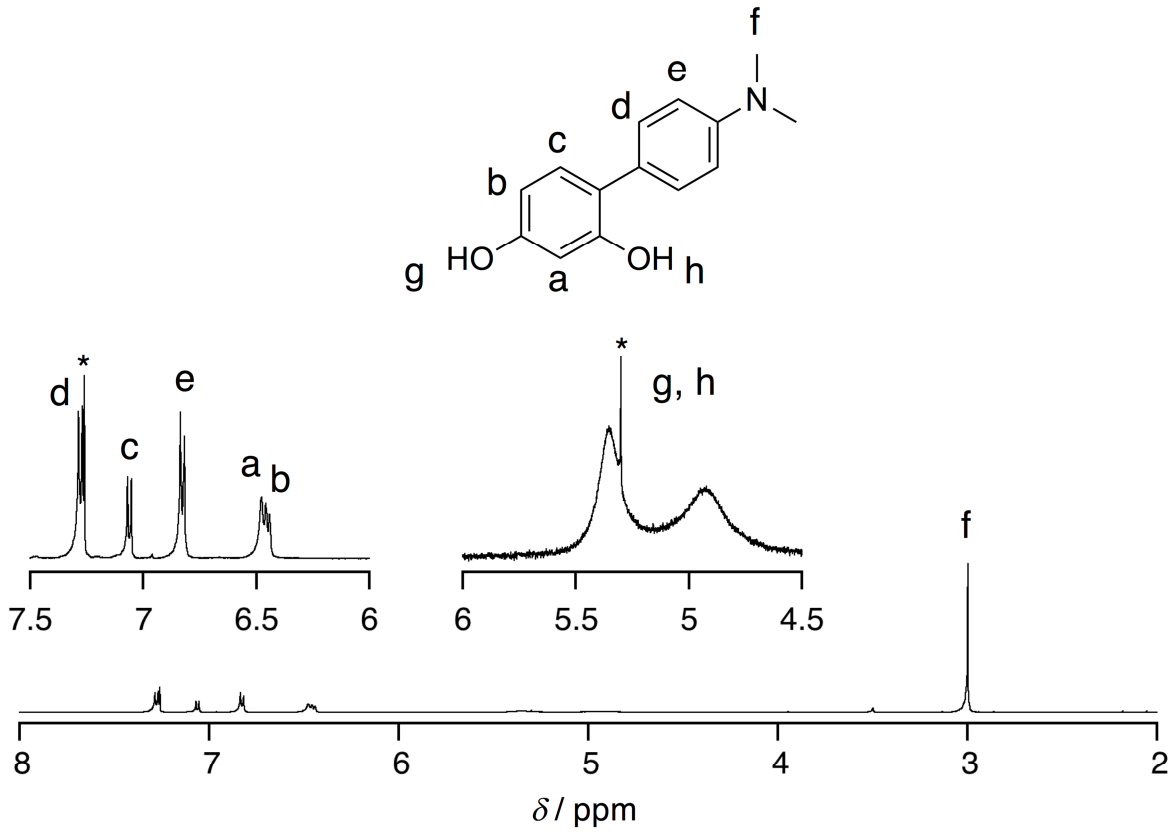

Figure S5. ^{1}H NMR spectrum of **4** in $CDCl_3$. *: solvents and impurities.

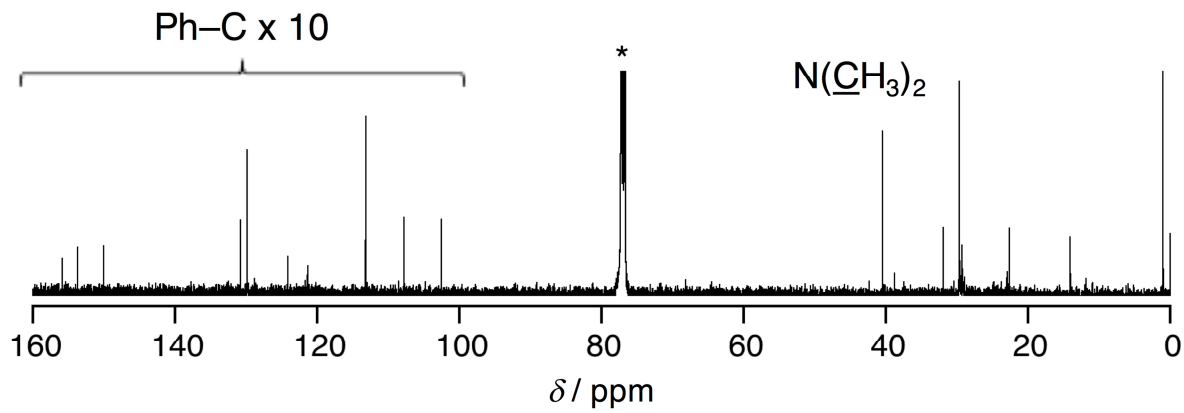

Figure S6. ^{13}C NMR spectrum of **4** in $CDCl_3$. *: solvents and impurities.

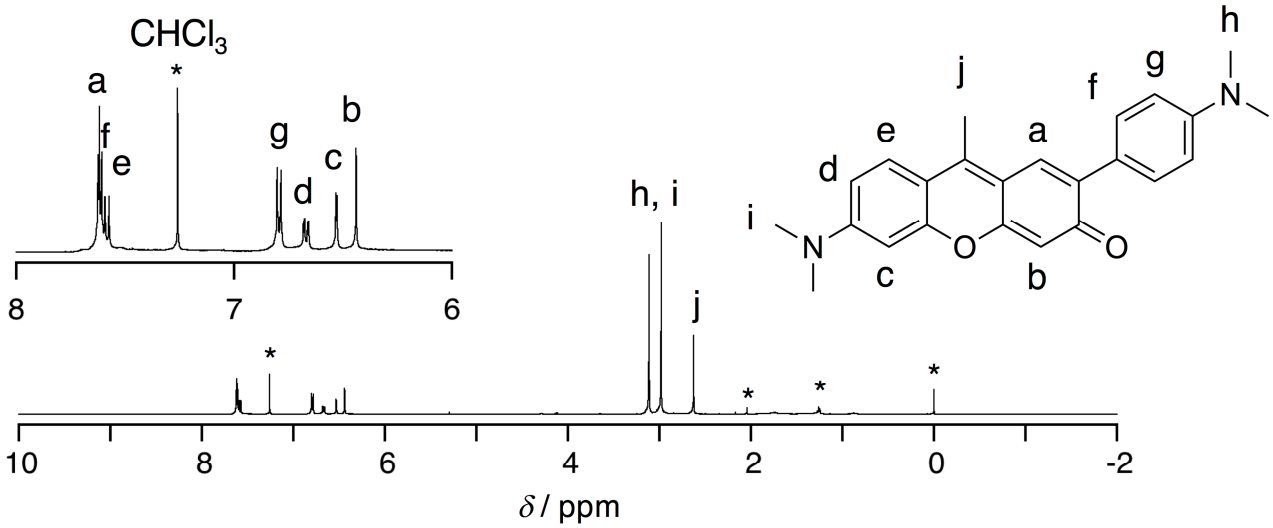

Figure S7. ^{1}H NMR spectrum of **6** in $CDCl_3$. *: solvents and impurities.

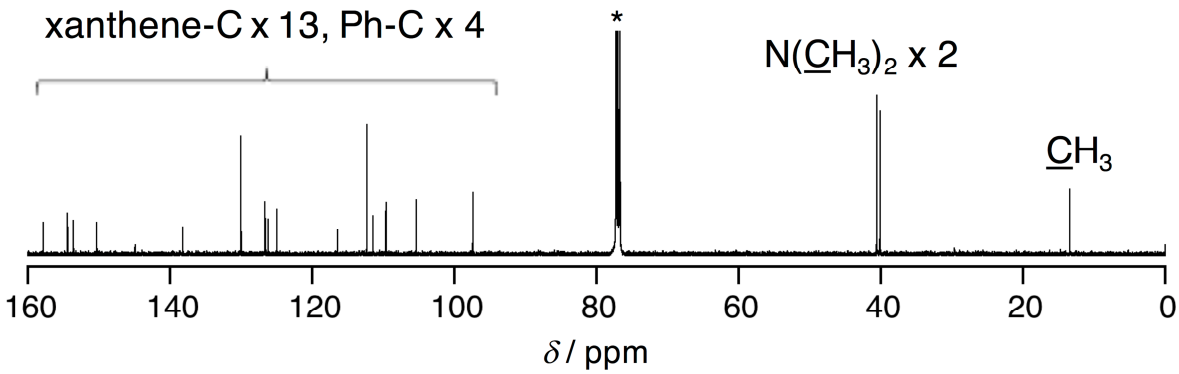

Figure S8. ^{13}C NMR spectrum of **6** in $CDCl_3$. *: solvents and impurities.

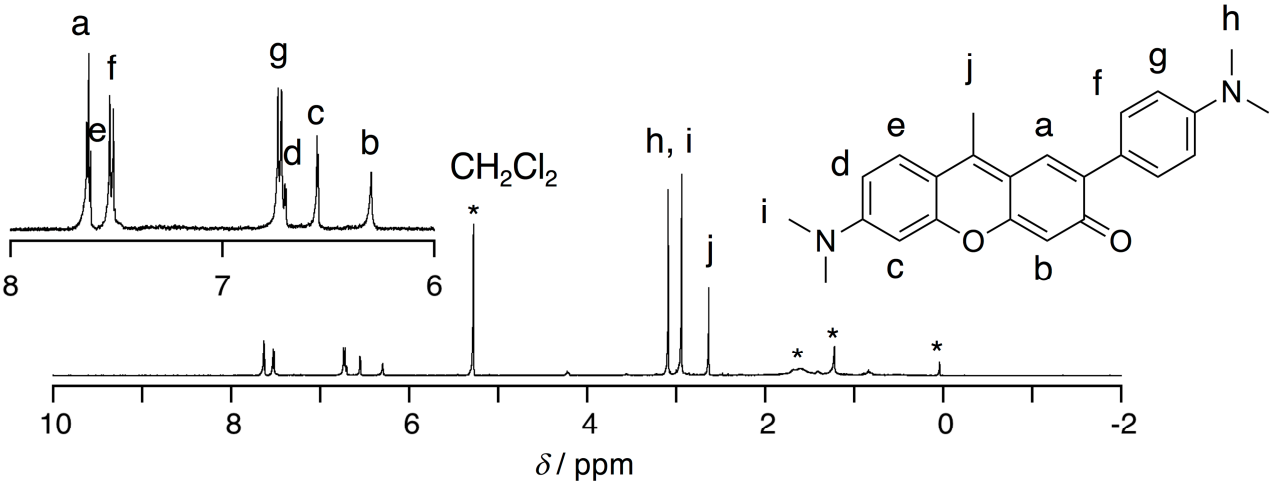

Figure S9. ^{1}H NMR spectrum of **6** in CD_2Cl_2. *: solvents and impurities.

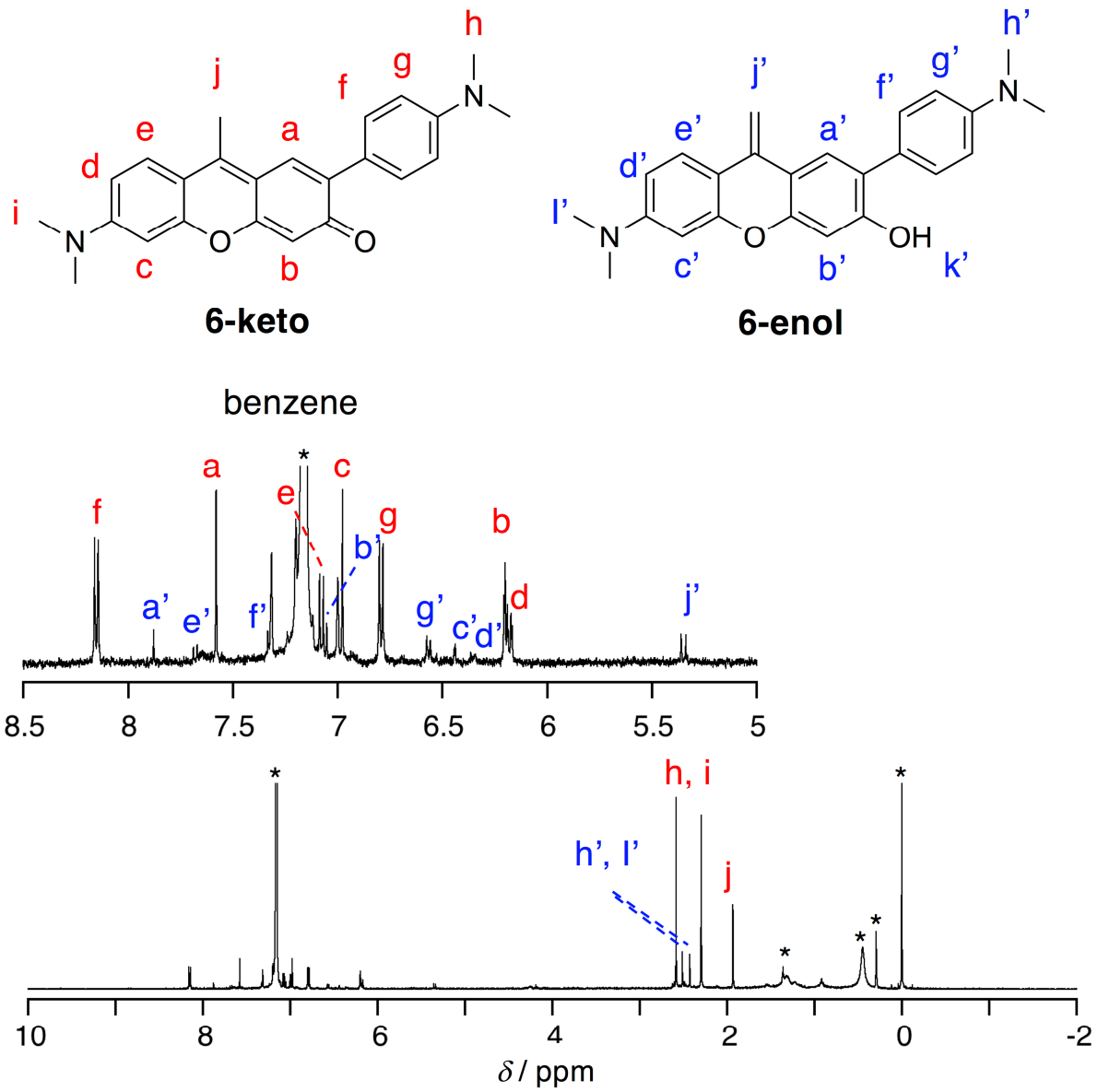

Figure S10. ^{1}H NMR spectrum of **6** in benzene-d_6. *: solvents and impurities.

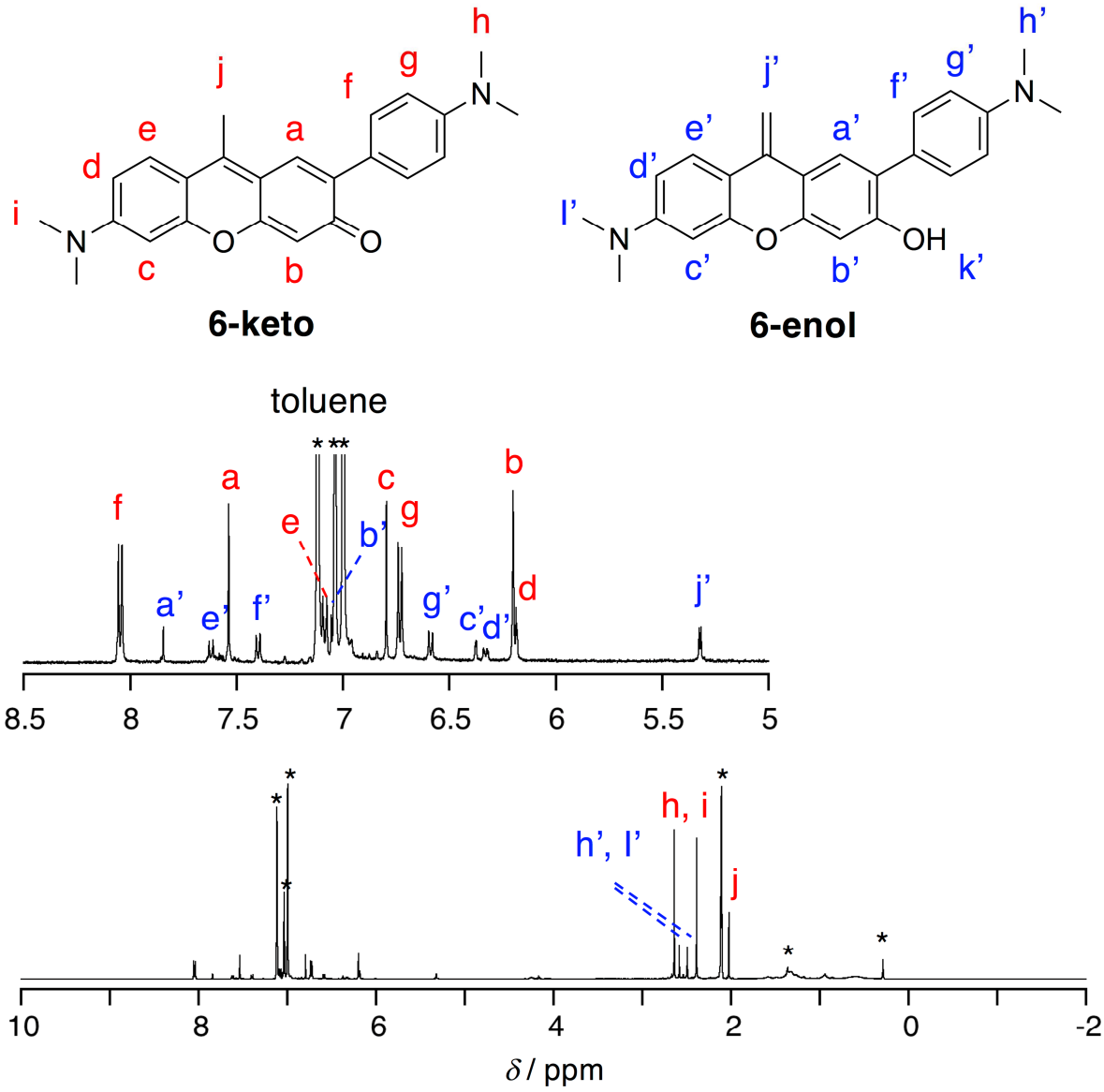

Figure S11. ^{1}H NMR spectrum of **6** in toluene-d_8. *: solvents and impurities.

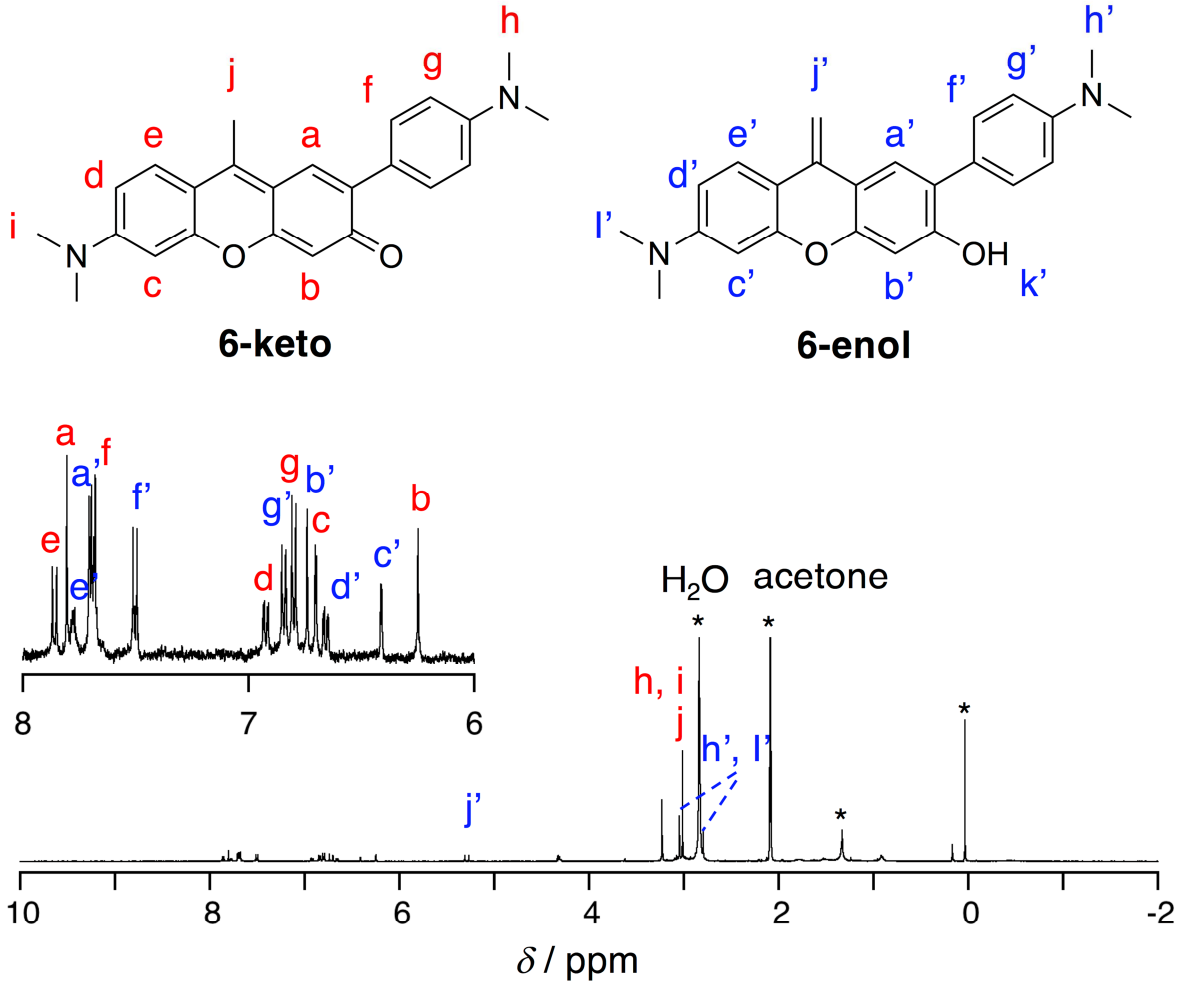

Figure S12. ^{1}H NMR spectrum of **6** in acetone-d_6. *: solvents and impurities.

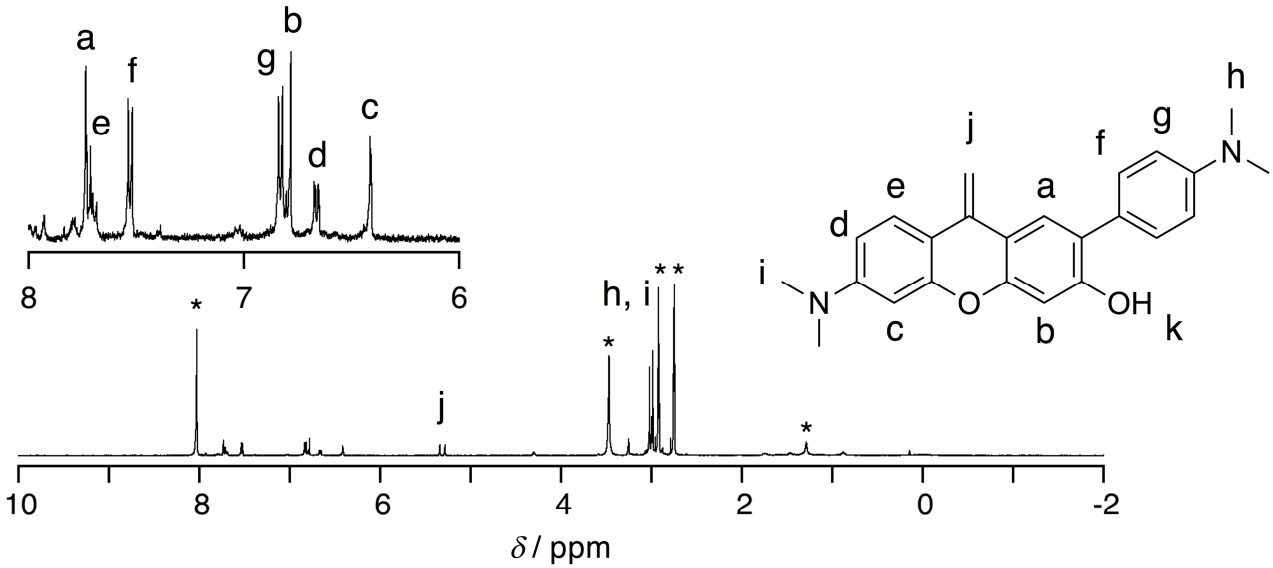

Figure S13. ^{1}H NMR spectrum of **6** in DMF-d_7. *: solvents and impurities.

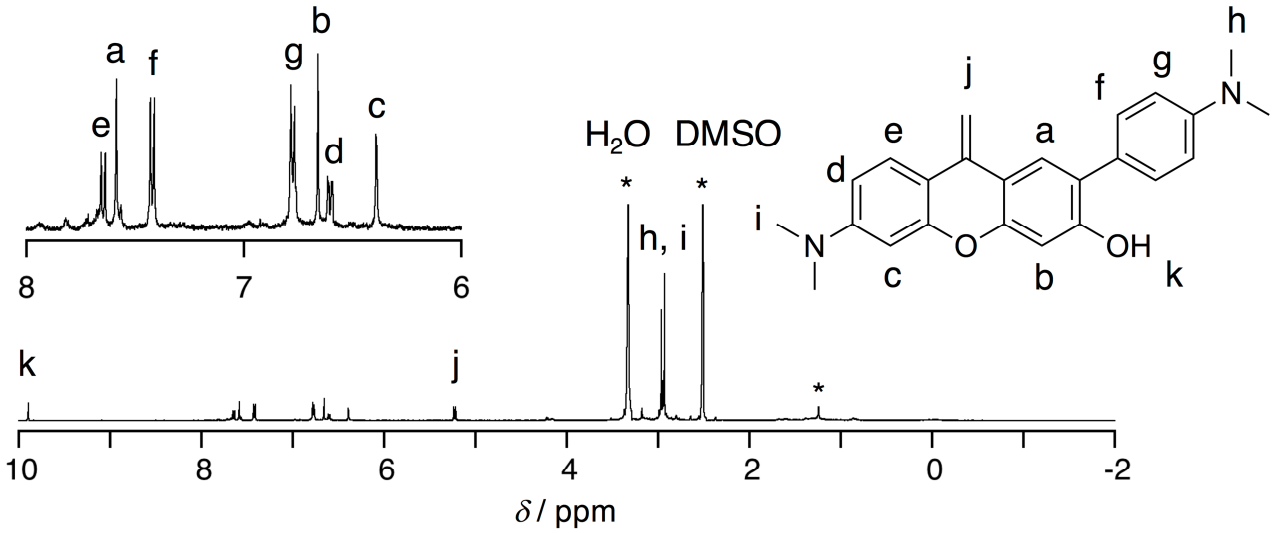

Figure S14. ^{1}H NMR spectrum of **6** in DMSO-d_6. *: solvents and impurities.

4. Absorption, emission and excitation spectra

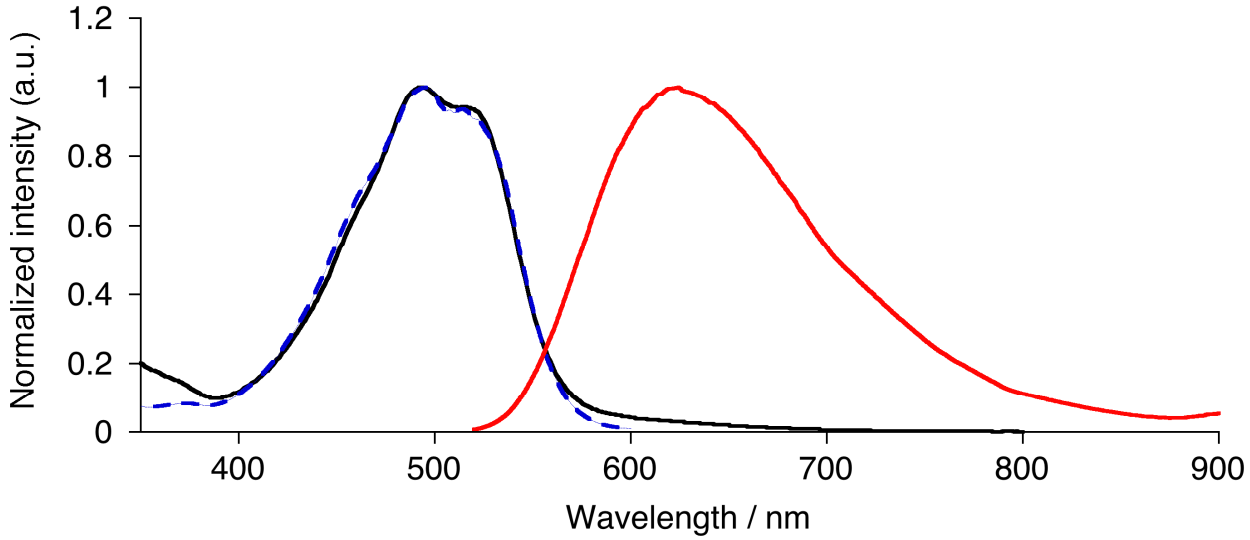

Figure S15. UV–vis absorption (black), fluorescence (red, excited at 490 nm), and excitation spectra of **6** (blue, dotted, monitored at 620 nm) in benzene.

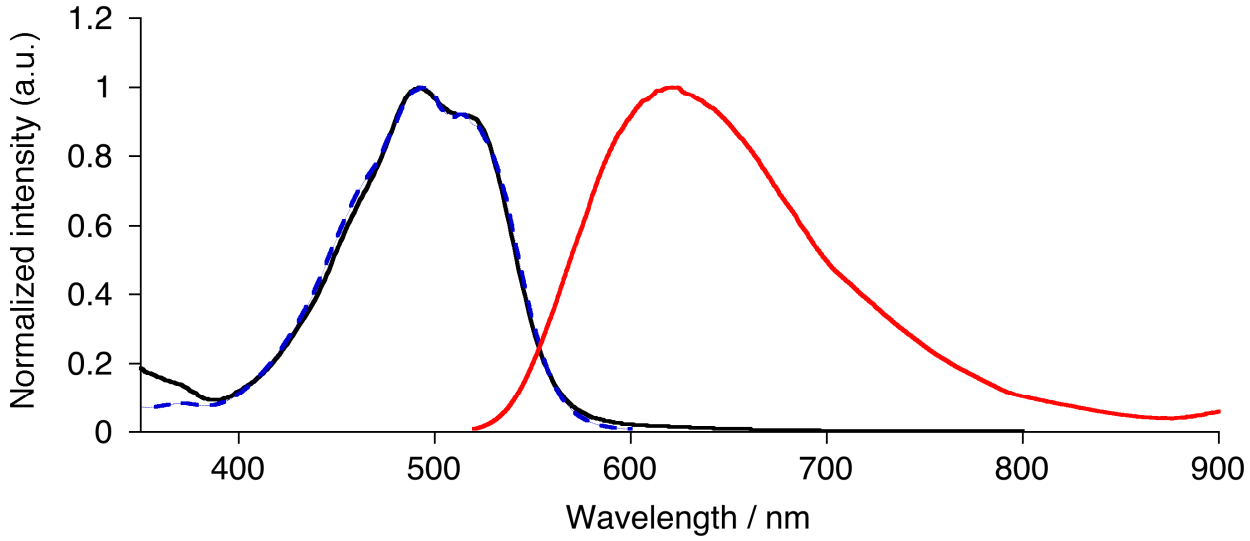

Figure S16. UV–vis absorption (black), fluorescence (red, excited at 490 nm), and excitation spectra of **6** (blue, dotted, monitored at 620 nm) in toluene.

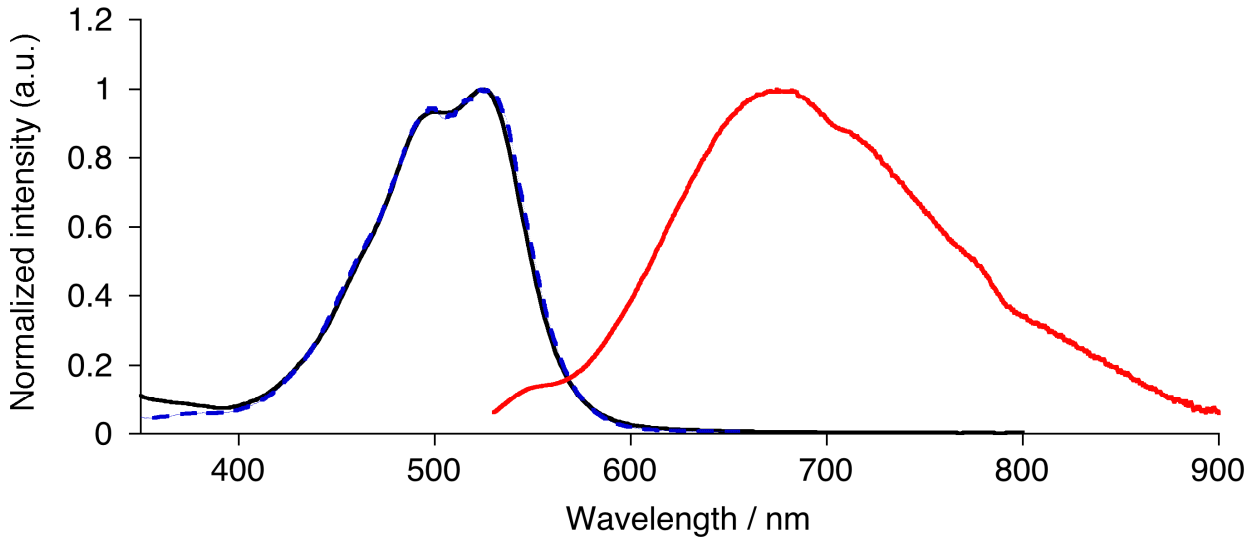

Figure S17. UV–vis absorption (black), fluorescence (red, excited at 515 nm), and excitation spectra of **6** (blue, dotted, monitored at 680 nm) in $CHCl_3$.

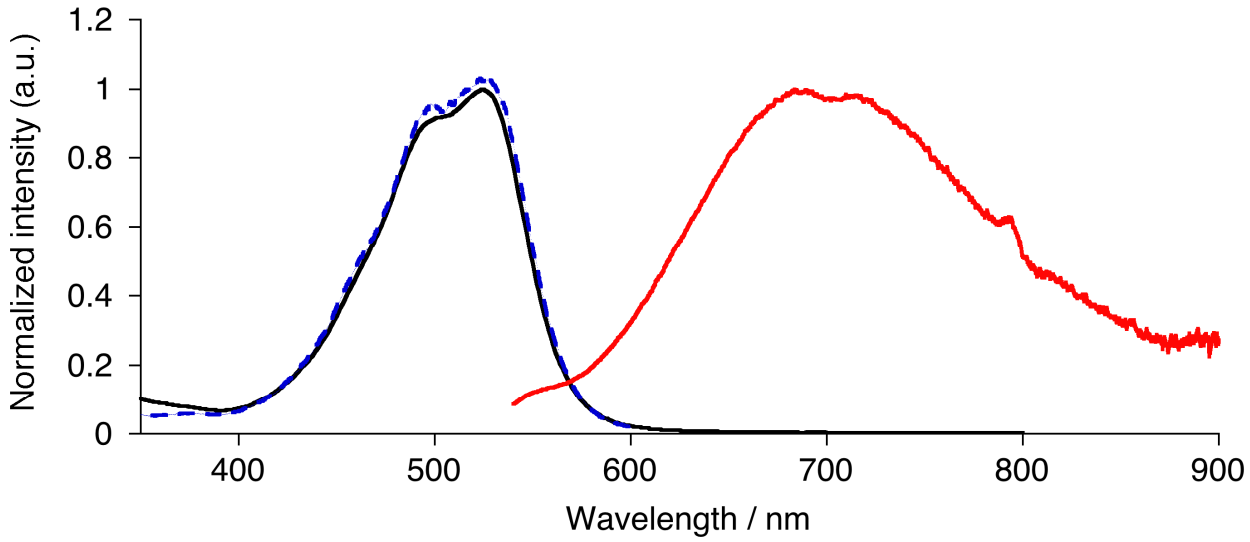

Figure S18. UV–vis absorption (black), fluorescence (red, excited at 525 nm), and excitation spectra of **6** (blue, dotted, monitored at 680 nm) in CH_2Cl_2.

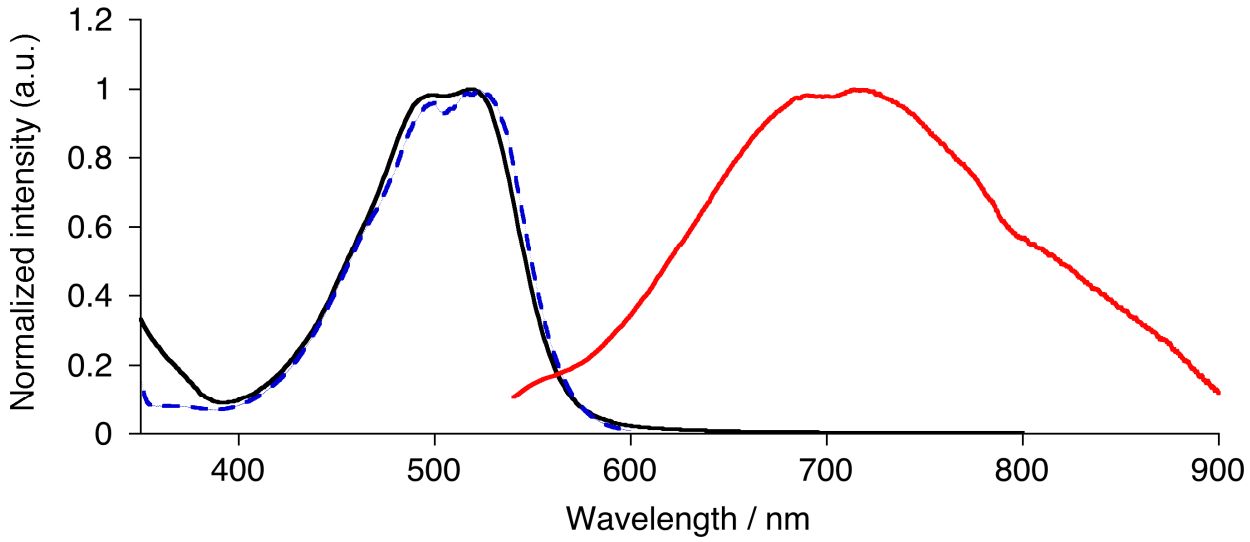

Figure S19. UV–vis absorption (black), fluorescence (red, excited at 525 nm), and excitation spectra of **6** (blue, dotted, monitored at 680 nm) in acetone.

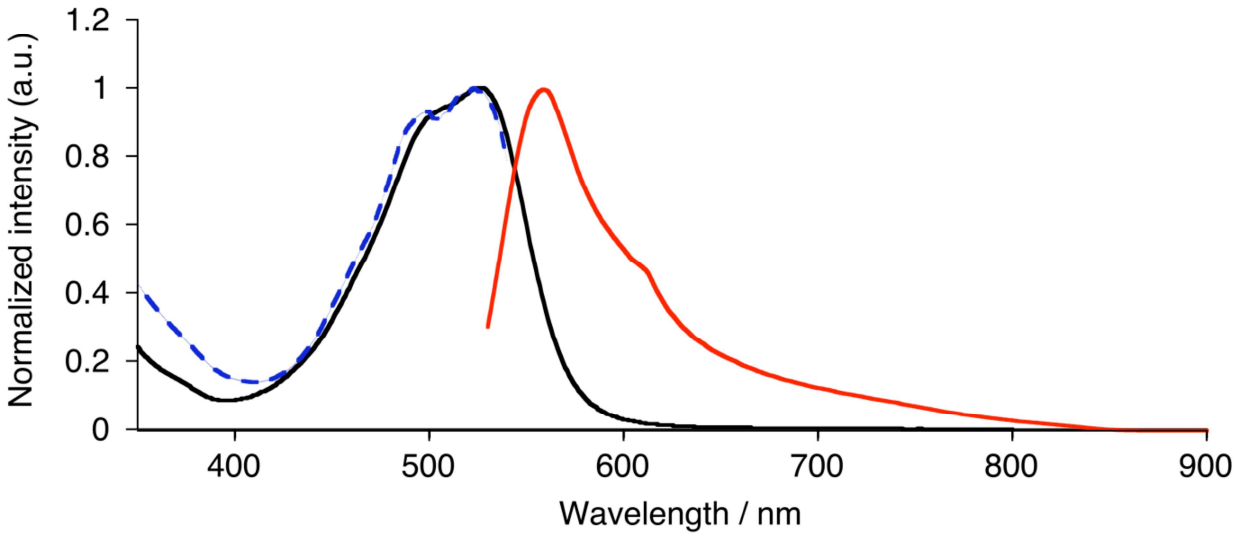

Figure S20. UV–vis absorption (black), fluorescence (red, excited at 520 nm), and excitation spectra of **6** (blue, dotted, monitored at 565 nm) in DMF.

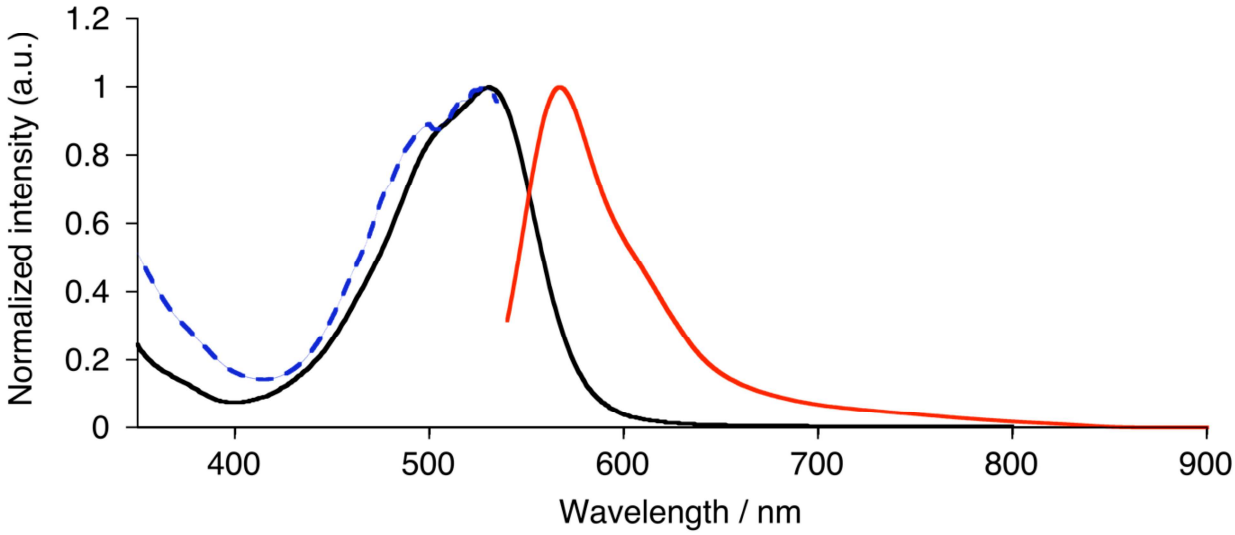

Figure S21. UV–vis absorption (black), fluorescence (red, excited at 532 nm), and excitation spectra of **6** (blue, dotted, monitored at 560 nm) in DMSO.

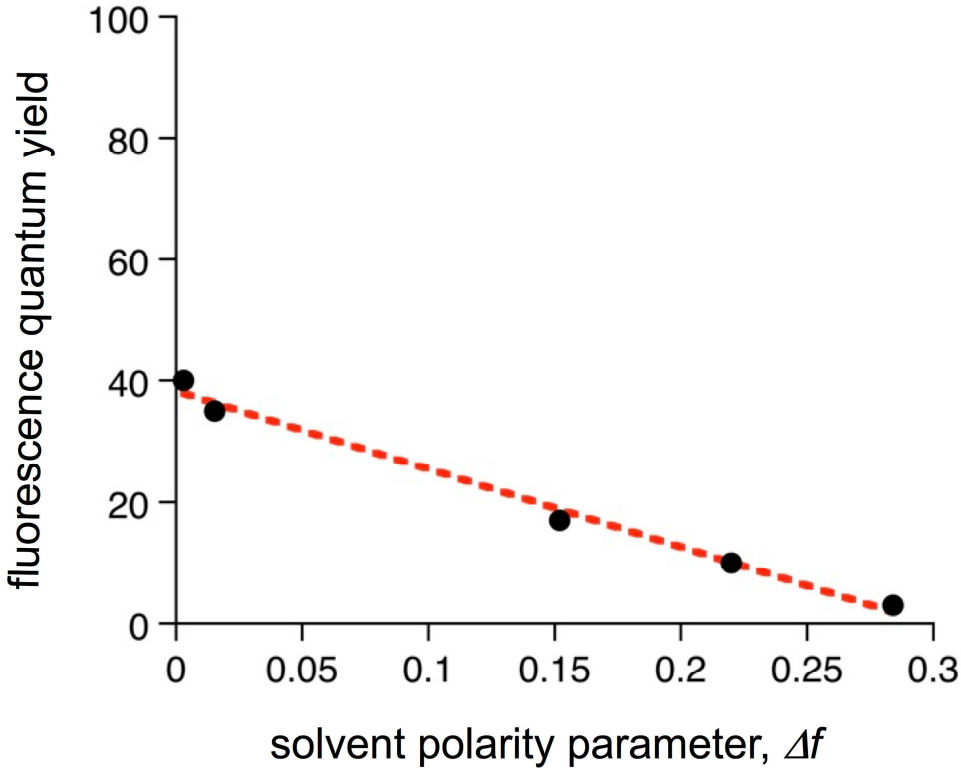

Figure S22. The plot of fluorescence quantum yield of **6** vs. solvent polarity parameter Δf for benzene, toluene, $CHCl_3$, CH_2Cl_2, and acetone.

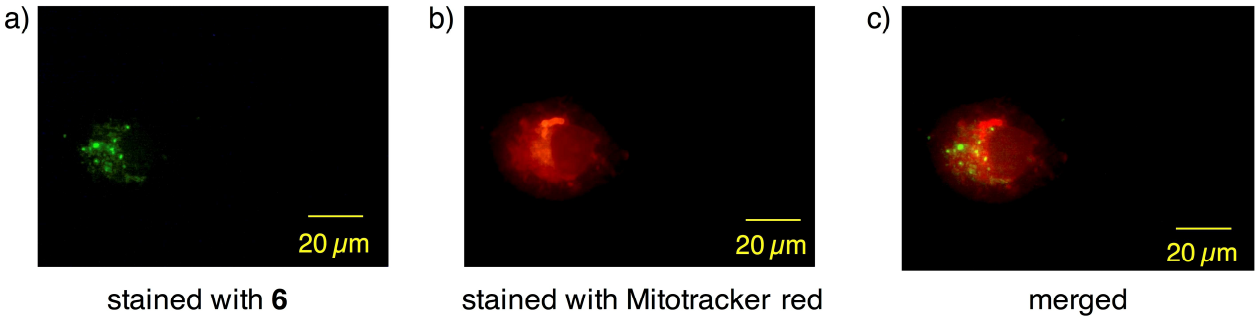

Figure S23. Fluorescence microscope images of living cells a) stained with **6**, b) stained with Mitotracker red, and c) the merged image.

5. Supporting references

[S1] G. R. Fulmer, A. J. M. Miller, N. H. Sherden, H. E. Gottlieb, A. Nudelman, B. M. Stoltz, J. E. Bercaw, K. I. Goldberg, *Organometallics* **2010**, *29*, 2176–2179.

Declaration of interests

☒ The authors declare that they have no known competing financial interests or personal relationships that could have appeared to influence the work reported in this paper.

☐The authors declare the following financial interests/personal relationships which may be considered as potential competing interests: